Rapid Communications

Coherent control of reactive scattering at low temperatures: Signatures of quantum interference in the differential cross sections for F + H_2 and F + HD

Adrien Devolder,[1] Timur Tscherbul,[2] and Paul Brumer[1]
[1]*Chemical Physics Theory Group, Department of Chemistry, and Center for Quantum Information and Quantum Control, University of Toronto, Toronto, Ontario, Canada M5S 3H6*
[2]*Department of Physics, University of Nevada, Reno, Nevada 89557, USA*

(Received 27 July 2020; accepted 1 September 2020; published 28 September 2020)

Fundamental entanglement related challenges have prevented quantum-interference-based control (i.e., coherent control) of collisional cross sections from being implemented in the laboratory. Here, differential cross sections for reactive scattering at low temperatures are shown to provide a unique opportunity to display such interference-based control by forming coherent superpositions of degenerate rotational states of reactant molecules $|jm\rangle$ with different m. In particular, we identify and quantify a unique signature of coherent control in reactive scattering with applications to F + H_2 → H + HF and HF + D ← F + HD → HD + F at 11 K. Control is shown to be extensive.

DOI: 10.1103/PhysRevA.102.031303

Coherent control of atomic and molecular processes (for a review until 2012, see [1]), i.e., the use of quantum interference to effect molecular outcomes, has proven enormously successful for certain classes of processes. These include light-induced control of unimolecular processes such as photodissociation [2], photoionization [3], control of currents in live brain cells [4], control of population transfer between system eigenstates [5], control of internal conversion [6], etc. By preparing multiple interfering pathways as initial states, primarily by laser excitation, quantum-interference-based control over various processes has been demonstrated both computationally (e.g., [1,7–9]) and experimentally (e.g., [2,3,10]). However, control over the wide class of collisional processes such as chemical reactions requires, in general, entanglement between the translation motion of the colliding partners and their internal degrees of freedom [1,11,12], a nontrivial experimental challenge for molecular collisional systems of interest. While this requirement can be relaxed for coherent control over the differential cross section (DCS) for A + BC collisions by forming coherent superpositions of energetically degenerate states of BC, coherent control of reactive scattering is yet to be demonstrated experimentally.

Such a demonstration would be particularly valuable for cold and ultracold chemical reactions in the quantum regime [13], which have become amenable to experimental studies owing to recent advances in cooling, trapping, and manipulating molecular gases [14]. These studies have revealed a number of fascinating phenomena, such as resonant scattering in cold He^* + H_2 [15,16] and He + NO [17] collisions, stereodynamics of H_2 + HD collisions at 1 K [18,19], quantum tunneling in the chemical reaction F + H_2 → HF + H at cold temperatures [20], and electric field control of the chemical reaction 2KRb → K_2 + Rb_2 at 50 nK [21,22]. Several theoretical studies explored the effects of molecular polarization [23] and alignment [24,25] on ultracold collision dynamics.

There are three primary motivations for using coherent control to manipulate cold molecular collisions. First, in the low-temperature regime the number of quantum states of the reactants (including partial waves for the relative motion) is dramatically reduced [13,14], minimizing thermal fluctuations and decoherence, and thereby enhancing quantum controllability of molecular processes. Second, because coherent control relies on the very general phenomenon of quantum interference, it could potentially be applied to a much wider range of molecular species than dc field control, which typically employs, e.g., Feshbach resonances to tune the scattering properties of ultracold atoms and molecules [26]. Thus, coherent control may prove advantageous in experimental settings where the presence of dc fields can cause undesirable perturbations, such as in precision measurements using atomic and molecular clocks [27,28]. Third, recent experimental studies of low-temperature collisions of molecules in single rotational states [17,20–22] and in superpositions thereof [18,19] now provide an experimental platform where such quantum-interference-based control of reactive scattering can be carried out.

Here we computationally demonstrate that (a) extensive control can be achieved over the DCS for reactive F + H_2 → HF + H, and F + HD → HF + D or DF + H in cold (11 K) scattering, by preparing a superposition of magnetic sublevels of *ortho*-H_2 and HD, and (b) that such control displays a unique measurable signature, readily identifying quantum interference as the basis for control. Computational results are obtained within a scenario that can be realized in modern experiments using merged beams of H_2 molecules created in superpositions of rotational states using, e.g., Stark-induced adiabatic Raman passage (SARP) [18,19]. The results also provide motivation for the extension to systems of particular interest in ultracold chemistry, such as those involving alkali-metal dimers KRb, NaK, and NaLi [21,29–31], and $^2\Sigma$ molecular radicals CaF, SrF, and SrOH [32–36].

We propose to control a reactive atom-molecule collision A + BC → AB + C by preparing an initial state $|\psi_s\rangle$ as a superposition of two m states of a diatomic molecule, a procedure that has been experimentally demonstrated using SARP [18,37,38]

$$|\psi_s\rangle = \cos(\eta)\,|1, v, j, m_1\rangle + \sin(\eta)\exp(i\beta)\,|1, v, j, m_2\rangle\,. \tag{1}$$

Here v and j are vibrational and rotational quantum numbers, respectively, and the first quantum number α corresponds to the chemical arrangement (i.e., A + BC, B +AC, or C + AB) with $\alpha = 1$ denoting the initial A + BC arrangement. The parameter η sets the relative population of the two states in the superposition with relative phase β.

Given this initial superposition state (1), the DCS to a final state (α', v', j', m'_j) can be written as the sum of two terms:

$$\sigma_{s\to\alpha' v' j' m'_j}(\theta,\phi) = \sigma^{\text{incoh}}_{s\to\alpha' v' j' m'_j}(\theta) + \sigma^{\text{int}}_{s\to\alpha' v' j' m'_j}(\theta,\phi), \tag{2}$$

where the subscript s denotes the initial superposition state [Eq. (1)]. The first of these terms, $\sigma^{\text{incoh}}_{s\to\alpha' v' j' m'_j}(\theta)$ is an incoherent contribution equivalent to the DCS from a mixture of m states with probabilities $\cos^2(\eta)$ and $\sin^2(\eta)$:

$$\sigma^{\text{incoh}}_{s\to\alpha' v' j' m'_j}(\theta) = \cos^2(\eta)|f_{1 v j m_1\to\alpha' v' j' m'_j}(\theta,\phi)|^2 + \sin^2(\eta)|f_{1 v j m_2\to\alpha' v' j' m'_j}(\theta,\phi)|^2, \tag{3}$$

where $f_{1 v j m_i\to\alpha' v' j' m'_j}(\theta,\phi,E)$ $(i = 1, 2)$ are the scattering amplitudes into product states $|\alpha' v' j', m'_j\rangle$ that are the key quantities to compute:

$$f_{\alpha v j m_j\to\alpha' v' j' m'_j}(\theta,\phi) = \frac{i\pi^{1/2}}{(k_{\alpha v j}k_{\alpha' v' j'})^{1/2}}\sum_{J,M}\sum_{\ell,\ell'}\sum_{m'_\ell} i^{\ell-\ell'}(2\ell+1)^{1/2}\begin{bmatrix} j & \ell & J\\ m_j & 0 & M\end{bmatrix}\begin{bmatrix} j' & \ell' & J\\ m'_j & m'_\ell & M\end{bmatrix} \times\left[\delta_{\alpha\alpha'}\delta_{v v'}\delta_{j j'}\delta_{\ell\ell'} - S^J_{\alpha v j l\to\alpha' v' j' l'}(E)\right]Y_{\ell' m'_\ell}(\theta,\phi). \tag{4}$$

Here, ℓ (ℓ') is the initial (final) partial wave and m_ℓ (m'_ℓ) is the initial (final) projection of $\vec{\ell}$ on the space-fixed quantization axis Z, E is the collision energy, and $k_{\alpha v j}$ ($k_{\alpha' v' j'}$) are the initial (final) relative momenta. The symbols in brackets are the Clebsch-Gordan (CG) coefficients, $Y_{\ell' m'_\ell}(\theta,\phi)$ are the spherical harmonics, and $S^J_{\alpha v j l\to\alpha' v' j' l'}(E)$ are the S-matrix elements.

The second term in Eq. (2), $\sigma^{\text{int}}_{s\to\alpha' v' j' m'_j}$, is the interference contribution, in which coherent control is manifest. Specifically, coherent control occurs via the quantum interference between the two scattering pathways arising from the initial m superposition (1). The interference term is then given by

$$\sigma^{\text{int}}_{s\to\alpha' v' j' m'_j}(\theta,\phi) = \cos(\eta)\sin(\eta)[e^{-i\beta}f_{1 v j m_1\to\alpha' v' j' m'_j}(\theta,\phi)f^*_{1 v j m_2\to\alpha' v' j' m'_j}(\theta,\phi) + e^{i\beta}f^*_{1 v j m_1\to\alpha' v' j' m'_j}(\theta,\phi)f_{1 v j m_2\to\alpha' v' j' m'_j}(\theta,\phi)]. \tag{5}$$

Note the characteristic difference between the direct terms [Eq. (4)] and the interference term [Eq. (5)]. Specifically, the latter shows a dependence of scattering on the azimuthal angle ϕ whereas the direct terms are ϕ independent. Hence, *ϕ-dependent scattering is a unique signature of interfering quantum pathways in the differential scattering cross section*. Previous experimental studies [18,19] on scattering with this type of superposition state did not measure this dependence insofar as detection included averaging over ϕ.

The ϕ dependence in Eq. (5) originates from the $e^{i m'_\ell\phi}$ term in the spherical harmonics contribution to the scattering amplitudes [see Eq. (4)]. The two CG coefficients in Eq. (4) ensure that $m'_\ell = m_j - m'_j$. Consequently, the scattering amplitudes can be written as $e^{i(m_j - m'_j)\phi}$ times a θ-dependent part:

$$f_{\alpha v j m_j\to\alpha' v' j' m'_j}(\theta,\phi) = e^{i(m_j - m'_j)\phi}|f_{\alpha v j m_j\to\alpha' v' j' m'_j}(\theta)|e^{i\xi_{\alpha v j m_j\to\alpha' v' j' m'_j}(\theta)}. \tag{6}$$

The products of the two scattering amplitudes in Eq. (5) are then proportional to $e^{i(m_1 - m_2)\phi}$. The interference term thus averages to zero when integrated over ϕ, which precludes coherent control over the integral cross sections (ICS) via a coherent superposition of a single reactant's $|jm\rangle$ states (1). (Control over the ICS for Penning and associative ionization is still possible, however, using a different scenario based on a coherent superposition of different m states of both reactants [12]). Inserting Eq. (6) into Eq. (5) gives the DCS for a final state as

$$\sigma_{s\to\alpha' v' j' m'_j}(\theta,\phi) = \sigma^{\text{incoh}}_{s\to\alpha' v' j' m'_j}(\theta) + 2\cos(\eta)\sin(\eta)|f_{\alpha v j m_1\to\alpha' v' j' m'_j}(\theta)||f_{\alpha v j m_2\to\alpha' v' j' m'_j}(\theta)| \times\cos[(m_1 - m_2)\phi + \Delta\xi(\theta) + \beta], \tag{7}$$

where $\Delta\xi(\theta) = \xi_{\alpha v j m_1\to\alpha' v' j' m'_j}(\theta) - \xi_{\alpha v j m_2\to\alpha' v' j' m'_j}(\theta)$ is the difference in the phase of the scattering amplitudes. The DCS for a specific final arrangement α', discussed below, is obtained by summing over all rovibrational states in this arrangement:

$$\sigma_{s\to\alpha'}(\theta,\phi) = \sigma^{\text{incoh}}_{s\to\alpha'}(\theta) + 2\cos(\eta)\sin(\eta)F_{s\to\alpha'}(\theta)\cos[(m_1 - m_2)\phi + \xi_{s\to\alpha'}(\theta) + \beta], \tag{8}$$

where $F_{s\to\alpha'}(\theta)$ and $\xi_{s\to\alpha'}(\theta)$ are, respectively, the magnitude and the phase of $\sum_{v',j',m_j'} f_{\alpha v j m_1\to\alpha' v' j' m_j'}(\theta,\phi) f^*_{\alpha v j m_2\to\alpha' v' j' m_j'}(\theta,\phi)$.

Equation (8) provides the central result of this work, which gives the DCS in terms of the scattering amplitude and the control parameters η and β of the initial coherent superposition of the reactant molecule's rotational states (1). Below, we expose the θ dependence of the cross section via the amplitude A, defined as

$$A(\eta,\theta) = 2\cos(\eta)\sin(\eta)F_{s\to\alpha'}(\theta). \tag{9}$$

Given an initial superposition state [Eq. (1)], control can be affected by varying the η and β parameters. Note that several structural features of the interference term are universal, i.e., independent of the system under consideration. These include the $e^{i(m_j-m_j')\phi}$ dependence on ϕ, the role of β as a phase in the DCS, and the dependence on η through $\cos(\eta)\sin(\eta)$. Below, we examine the case of a symmetric superposition ($\eta=\pi/4$), which gives the maximum value of $\cos(\eta)\sin(\eta)$, and set $\beta=0$ since variations in β just correspond to a shift in phase of the interference term. We emphasize below the ϕ dependence of the cross sections because it is a unique signature of quantum interference contribution to the scattering. The extent of this contribution can be quantified via the visibility $\mathcal{V}(\theta)$ manifest here as the difference between the maximum and minimum DCSs as a function of ϕ, scaled by the sum of both

$$\mathcal{V}(\theta) = \frac{\sigma^{\max(\phi)}_{s\to\alpha' v' j' m_j'}(\theta,\phi) - \sigma^{\min(\phi)}_{s\to\alpha' v' j' m_j'}(\theta,\phi)}{\sigma^{\max(\phi)}_{s\to\alpha' v' j' m_j'}(\theta,\phi) + \sigma^{\min(\phi)}_{s\to\alpha' v' j' m_j'}(\theta,\phi)}. \tag{10}$$

From Eqs. (8) and (9), we obtain the visibility as the ratio $A(\theta)/\sigma^{\text{incoh}}_{s\to\alpha'}(\theta)$. Indeed, the extent to which coherent control is significant is dictated by the relative magnitude of the amplitude A and the incoherent contributions, i.e., by the visibility $\mathcal{V}$ of the interference fringes. For the case of two pathways, $\mathcal{V}$ satisfies [39,40]

$$\mathcal{P}(\theta)^2 + \mathcal{V}(\theta)^2 \leqslant 1, \tag{11}$$

an expression of wave-particle duality, with $\mathcal{V}$ measuring the wavelike behavior and $\mathcal{P}(\theta)$ is the path distinguishability [40]. The highest value for the visibility $\mathcal{V}$ is then 1, corresponding to a situation where the two pathways are completely indistinguishable. The closer it is to unity, the greater the contribution of the interfering indistinguishable pathways to the scattering. Note that the positivity of the DCS implies that $A \leqslant \sigma^{\text{incoh}}_{s\to\alpha'}(\theta)$, which is consistent with the unitary limit for the visibility.

We now apply the methodology developed above to explore the possibility of controlling cold chemical reactions $F + H_2 \to HF + H$ and $F + HD \to H + DF$ and $D + HF$, whose quantum dynamics has been the subject of many theoretical studies [20,41–49]. Recent experimental advances in preparing coherent superpositions of rotational states of H_2 [18,19] and in reactive scattering of $F + H_2$ at 11 K [20] indicate the feasibility of an experiment (the first coherent control experiment of reactive scattering) of the kind motivated by the results below. The reaction DCSs are computed using Eqs. (2)–(5) parametrized by the S-matrix elements obtained via a numerically exact time-independent quantum reactive scattering approach [50]. The S-matrix elements were calculated by solving the coupled-channel (CC) scattering equations in hyperspherical coordinates using the ABC code [50] based on the Stark-Werner potential energy surface (PES) ([51]). Calculations were carried out at an incident collision energy of 11 K, for the total angular momenta $J = 0$–7 and for the inversion parities $\epsilon = +1$ (for $J = 0$) and $\epsilon = \pm 1$ (for $J > 0$). The CC equations were propagated to a maximal hyperradius of $\rho_{\max} = 40$ a.u. in steps of $\Delta\rho = 0.01$ a.u. A cut-off energy of 2.5 eV for the rovibrational basis sets was imposed, with a maximum of 15 diatomic rotational levels. $k_{\max}$ is fixed at 4 for $J < 5$ while it is equal to J for $J > 5$. The calculated S-matrix elements are obtained in the body-fixed coordinate frame (BFF) and then transformed to the space-fixed frame (SFF). The transformation matrix between the BFF and SFF is given by diagonalizing the operator $\hat{L}^2$, $\vec{L}$ being the orbital angular momentum of the collisional complex. The calculated S-matrix elements and reaction probabilities were converged to 10%. As a further test, we compared the energy dependence of the $F + H_2$ reaction probabilities between 1 and 10 K with the previous calculations employing the same PES [42] and found good agreement.

From the S matrix in the SFF, we calculated the scattering amplitudes $f_{\alpha v j m_j\to\alpha' v' j' m_j'}(\theta,\phi,E)$ using Eq. (4). The DCSs were calculated in two different ways. First, we used Eqs. (2), (3), and (5), summed over all rovibrational levels in a given arrangement. Second, we calculated the DCS through Eq. (8) using the quantity $F_{s\to\alpha'}(\theta)$ and the phase ξ via the module and argument of $\sum_{v',j',m_j'} f_{\alpha v j m_1\to\alpha' v' j' m_j'}(\theta,\phi) f^*_{\alpha v j m_2\to\alpha' v' j' m_j'}(\theta,\phi)$. The two methods give the same DCS. Finally, for the cases without superposition ($\eta = 0$ and $\eta = \pi/2$), we compared the calculated DCS with the code provided by Dr. D. De Fazio, again finding good agreement.

We note that (1) our calculations neglect the fine-structure effects due to the open-shell nature of the fluorine atom, and (2) the underlying Stark-Werner PES is known to overestimate the $F + H_2$ reaction rates at 11 K by a factor of $\simeq 3$. These quantitative inaccuracies are unlikely to affect the qualitative results of this work, which show efficient coherent control of the DCS and the HF + D/DF + H product branching ratios, and can therefore be used to establish qualitative trends in controlling low-temperature reaction rates, the main goal of this work. More extensive models including spin-orbit effects and nonadiabatic coupling [41,46,49] could be considered in future work, if motivated by experimental studies.

We consider two different m superpositions of the magnetic sublevels of the first excited rotational state ($j = 1$) of the vibrational ground state ($v = 0$) of either *ortho*-H_2 or HD. The first superposition, between $m_1 = -1$ and $m_2 = 0$, is denoted $-1/0$ and the second, between $m_1 = -1$ and $m_2 = +1$, is denoted $-1/+1$.

The calculated DCS for the $F + H_2(-1/0) \to HF + H$ reaction is shown in Fig. 1(a) as a function of θ and ϕ. Although the interference contribution affects both the dependence on θ and ϕ, the explicit ϕ-dependent signature of interference at the θ value, for which the DCS is maximal (here, $\theta = 0.65\pi$) is shown in Fig. 1(b). The ϕ dependence of the DCS is seen to oscillate about the direct term, with a frequency equal to the difference of the projections of magnetic sublevels in the

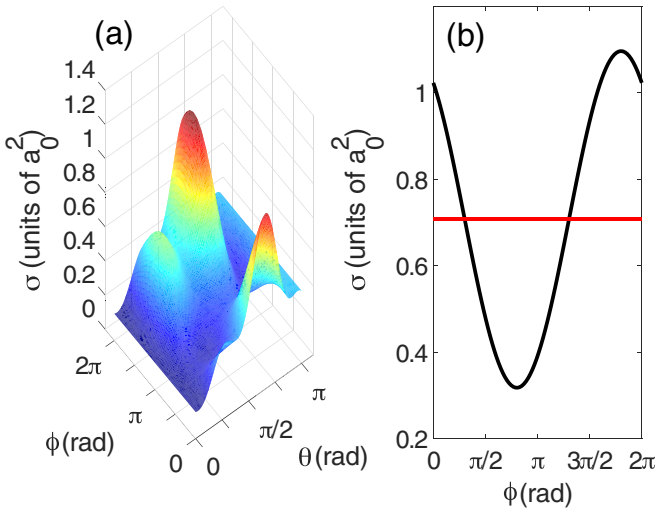

FIG. 1. Reactive DCS for F + H_2 at 11 K with the initial superposition $-1/0$ ($\eta = \pi/4$ and $\beta = 0$). (a) Three-dimensional (3D) plot representing the θ and ϕdependences of the DCS. (b) ϕ dependence at fixed θ ($\theta = 0.65\pi$ rad). The DCS is plotted in black while the incoherent contribution is plotted in red (gray). Similar control results are obtained at 1 K.

superposition (1), as anticipated from Eq. (8). A simple computation gives $\mathcal{V} = 0.54$, whose square, ≈ 0.33, constitutes a considerable interference contribution.

Whereas the functional form (albeit not the magnitude) of the ϕ dependence of the DCS given by $\exp[i(m - m')\phi]$ is universal, the θ dependence of the amplitude A (9), of the incoherent contribution (3) and therefore of the visibility (10) are system dependent. Figure 2(a) shows the θ dependence of the visibility for the F + H_2 superpositions $-1/0$ and $-1/+1$. No clear advantage of one superposition over the other appears, with the maximal visibility $\mathcal{V}_{\max} = 0.54$. The interference clearly vanishes in the forward and backward directions, where the scattering amplitudes are zero.

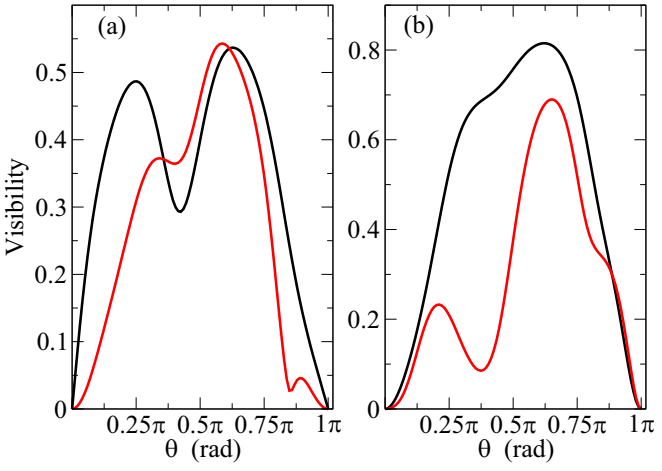

FIG. 2. θ dependence of the visibility for (a) F + H_2 → HF + H with the initial superpositions $-1/0$ (black) and $-1/+1$ [red (gray)], and for (b) F + HD → DF + H (black) and HF + D [red (gray)] with the initial superpositions $-1/+1$.

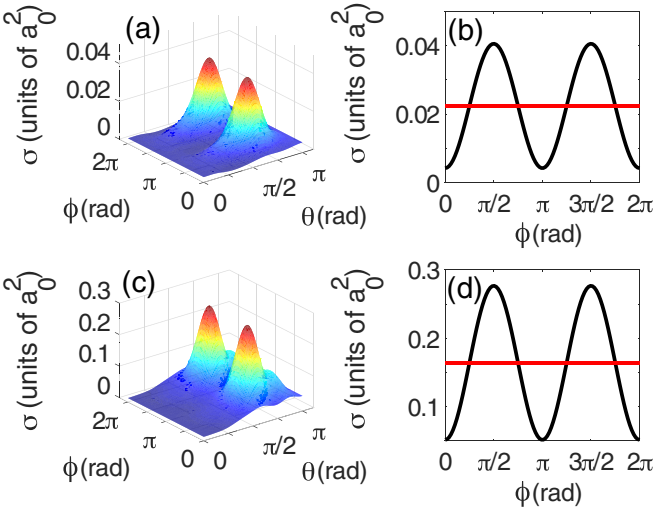

FIG. 3. Reactive DCS for F + HD at 11 K with the initial superposition $-1/+1$ ($\eta = \pi/4$ and $\beta = 0$). (a) and (c) 3D plot of the θ- and ϕ-dependent DCS. (b) and (d) ϕ dependence of the DCS at $\theta = 0.64\pi$. Panels (a) and (b) correspond to the reactive channel DF + H while panels (c) and (d) correspond to the reactive channel HF + D. The DCS are plotted in black while the incoherent contributions are plotted in red (gray). Note the difference in ordinate scale for the two different products. Similar control results are obtained at 1 K.

Similarly to the amplitude $A(\theta)$, the phase $\xi_{s\to\alpha'}(\theta)$ of DCS oscillations (8), given by the difference of phases of scattering amplitudes, is system dependent. The phase is particularly sensitive to the presence of a symmetry between the different components of the superposition (1). For example, the two states of the superposition $-1/+1$ are related by the time-reversal symmetry and the phase ξ of the DCS oscillations is zero for all θ. Inversely, for the superposition $-1/0$, we observe a θ-dependent phase $\xi(\theta)$ of the DCS oscillations [see, e.g., Fig. 1(b)]. Thus, by measuring the angular dependence of the DCS for molecules reacting in quantum superposition states (1), it is possible to infer information not only about the magnitude, but also about the phase of the scattering amplitudes.

Control over reactive F + HD scattering presents additional challenges and opportunities, insofar as successful control should be able to *selectively distinguish* between the H + FD and D + HF product channels. Figure 3 shows the results for controlling the individual DCSs for each of the product channels with the initial superposition $-1/+1$. Extensive ϕ dependences for both reactive channels are evident with large visibility, $\mathcal{V} = 0.81$ for the H + DF channel, and 0.69 for the H + FD channel. Note that the DCS is larger for D + HF than for the DF + H channel, a consequence of faster tunneling of the hydrogen atom.

The vanishing of the phases $\xi(\theta)$ for both of the product channels [see Figs. 3(b) and 3(d)] due to time-reversal symmetry implies that the selectivity in the control over these channels can only arise from differences in the θ dependence of the visibilities $\mathcal{V}$ shown in Fig. 2(b). We observe that the best selectivity is expected for $\theta = \pi/4 - \pi/2$ rather than at the maximum of the visibilities, where the θ dependence is similar for both of the product channels. To further reveal this

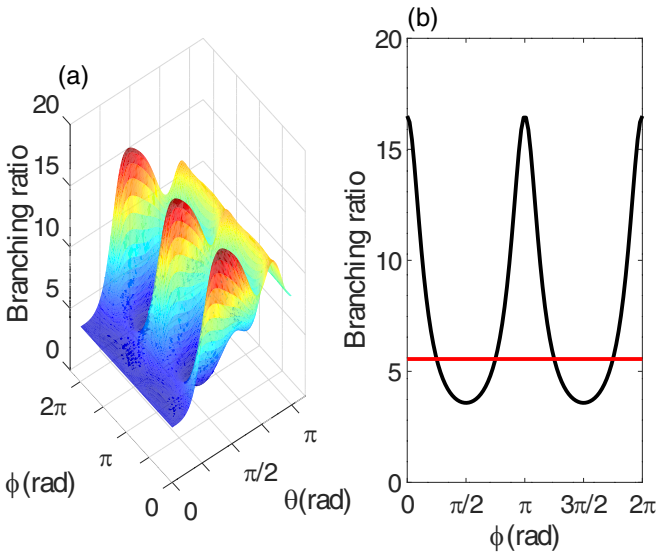

FIG. 4. Differential branching ratio (HF + D)/DF + H) of the DCS between the reactive channels for F+HD with the initial superposition $-1/1$. (a) 3D surface plot of the θ and ϕ dependences of the DCS. (b) ϕ dependence of the branching ratio at a fixed $\theta = 0.47\pi$. The differential branching ratio is plotted in black while the incoherent contribution is plotted in red (gray).

selectivity, we plot in Fig. 4 the differential branching ratio, the ratio of the DCS $\sigma(\theta, \phi)$ for the two product channels HF + D and DF + H. The ϕ dependence of the ratio shown in Fig. 4(b) is seen to vary over a wide range, from 3.6 to 16.5, clearly demonstrating interference-based *product channel selectivity* with interference quantified at $\mathcal{V} = 0.64$. We note that since the ϕ dependence of the HF + D/DF + H branching ratio is given by the ratio of two in-phase oscillations, it is not symmetric about the ratio of incoherent contributions shown by the horizontal line in Fig. 4(b).

In summary, we have computationally demonstrated extensive quantum-interference-based coherent control over low-temperature differential scattering in the F + H_2 and F + HD chemical reactions using an approach that is experimentally feasible. Quantum interference control is manifest explicitly in a signature experimental observable, the nonzero ϕ dependence of the scattering. The successful experimental demonstration of this control would open the entire class of scattering processes to coherent control.

The proposed control scenario is completely general and can be extended to all reactive scattering processes of interest to ultracold chemistry. Significantly, this scheme allows for controlling chemical reactions that are not readily susceptible to traditional electric and magnetic field control, such as those involving homonuclear ground-state alkali-metal dimers [52–55] and H_2, the most abundant molecule in the Universe and one of the very few molecules, whose reaction dynamics can be studied theoretically with spectroscopic accuracy [16,56–58]. Furthermore, because ϕ-dependent interference is observed only if the atom-molecule PES is anisotropic, this dependence provides direct insight into the angular dependence of the PES. Measuring the ϕ-dependent DCS in a coherently controlled cold scattering experiment could, therefore, serve a useful probe of the interaction anisotropy in atom-molecule reactive scattering.

This work was supported by the U.S. Air Force Office for Scientific Research (AFOSR) under Contract No. FA9550-19-1-0312. SciNet computational facilities are gratefully acknowledged, as are discussions with Prof. Millard Alexander. We thank Dr. Dario De Fazio for providing his test code for the calculation of DCSs.

[1] M. Shapiro and P. Brumer, *Quantum Control of Molecular Processes* (Wiley-VCH, Weinheim, 2012).
[2] B. Sheehy, B. Walker, and L. F. DiMauro, Phys. Rev. Lett. **74**, 4799 (1995).
[3] L. Zhu, V. Kleiman, X. Li, S. P. Lu, K. Trentelman, and R. J. Gordon, Science **270**, 77 (1995).
[4] C. Lavigne and P. Brumer, J. Chem. Phys. **153**, 034303 (2020).
[5] V. D. Kleiman, L. Zhu, X. Li, and R. J. Gordon, J. Chem. Phys. **102**, 5863 (1995).
[6] T. Grinev, M. Shapiro, and P. Brumer, J. Phys. B **48**, 174004 (2015).
[7] P. Brumer and M. Shapiro, Chem. Phys. Lett. **126**, 541 (1986).
[8] P. Brumer and M. Shapiro, Faraday Discuss. Chem. Soc. **82**, 177 (1986).
[9] D. J. Tannor and S. A. Rice, J. Chem. Phys. **83**, 5013 (1985).
[10] A. Shnitman, I. Sofer, I. Golub, A. Yogev, M. Shapiro, Z. Chen, and P. Brumer, Phys. Rev. Lett. **76**, 2886 (1996).
[11] M. Shapiro and P. Brumer, Phys. Rev. Lett. **77**, 2574 (1996).
[12] J. J. Omiste, J. Floß, and P. Brumer, Phys. Rev. Lett. **121**, 163405 (2018).
[13] R. V. Krems, Phys. Chem. Chem. Phys. **10**, 4079 (2008).
[14] J. L. Bohn, A. M. Rey, and J. Ye, Science **357**, 1002 (2017).
[15] A. B. Henson, S. Gersten, Y. Shagam, J. Narevicius, and E. Narevicius, Science **338**, 234 (2012).
[16] A. Klein, Y. Shagam, W. Skomorowski, P. S. Żuchowski, M. Pawlak, L. M. C. Janssen, N. Moiseyev, S. Y. T. van de Meerakker, A. van der Avoird, C. P. Koch, and E. Narevicius, Nat. Phys. **13**, 35 (2016).
[17] S. N. Vogels, J. Onvlee, S. Chefdeville, A. van der Avoird, G. C. Groenenboom, and S. Y. T. van de Meerakker, Science **350**, 787 (2015).
[18] W. E. Perreault, N. Mukherjee, and R. N. Zare, Science **358**, 356 (2017).
[19] W. E. Perreault, N. Mukherjee, and R. N. Zare, Nat. Chem. **10**, 561 (2018).
[20] M. Tizniti, S. D. L. Picard, F. Lique, C. Berteloite, A. Canosa, M. H. Alexander, and I. R. Sims, Nat. Chem. **6**, 141 (2014).
[21] K.-K. Ni, S. Ospelkaus, D. Wang, G. Quéméner, B. Neyenhuis, M. H. G. de Miranda, J. L. Bohn, J. Ye, and D. S. Jin, Nature (London) **464**, 1324 (2010).

[22] M. H. G. de Miranda, A. Chotia, B. Neyenhuis, D. Wang, G. Quéméner, S. Ospelkaus, J. L. Bohn, J. Ye, and D. S. Jin, Nat. Phys. **7**, 502 (2011).
[23] J. Aldegunde, J. M. Alvariño, M. P. de Miranda, V. Sáez Rábanos, and F. J. Aoiz, J. Chem. Phys. **125**, 133104 (2006).
[24] J. F. E. Croft, N. Balakrishnan, M. Huang, and H. Guo, Phys. Rev. Lett. **121**, 113401 (2018).
[25] P. G. Jambrina, J. F. E. Croft, H. Guo, M. Brouard, N. Balakrishnan, and F. J. Aoiz, Phys. Rev. Lett. **123**, 043401 (2019).
[26] C. Chin, R. Grimm, P. Julienne, and E. Tiesinga, Rev. Mod. Phys. **82**, 1225 (2010).
[27] A. Derevianko and H. Katori, Rev. Mod. Phys. **83**, 331 (2011).
[28] A. D. Ludlow, M. M. Boyd, J. Ye, E. Peik, and P. O. Schmidt, Rev. Mod. Phys. **87**, 637 (2015).
[29] S. Ospelkaus, K.-K. Ni, D. Wang, M. H. G. de Miranda, B. Neyenhuis, G. Quéméner, P. S. Julienne, J. L. Bohn, D. S. Jin, and J. Ye, Science **327**, 853 (2010).
[30] J. W. Park, S. A. Will, and M. W. Zwierlein, Phys. Rev. Lett. **114**, 205302 (2015).
[31] T. M. Rvachov, H. Son, A. T. Sommer, S. Ebadi, J. J. Park, M. W. Zwierlein, W. Ketterle, and A. O. Jamison, Phys. Rev. Lett. **119**, 143001 (2017).
[32] J. F. Barry, D. J. McCarron, E. B. Norrgard, M. H. Steinecker, and D. DeMille, Nature (London) **512**, 286 (2014).
[33] D. J. McCarron, M. H. Steinecker, Y. Zhu, and D. DeMille, Phys. Rev. Lett. **121**, 013202 (2018).
[34] L. W. Cheuk, L. Anderegg, B. L. Augenbraun, Y. Bao, S. Burchesky, W. Ketterle, and J. M. Doyle, Phys. Rev. Lett. **121**, 083201 (2018).
[35] L. Anderegg, B. L. Augenbraun, Y. Bao, S. Burchesky, L. W. Cheuk, W. Ketterle, and J. M. Doyle, Nat. Phys. **14**, 890 (2018).
[36] I. Kozyryev, L. Baum, K. Matsuda, B. L. Augenbraun, L. Anderegg, A. P. Sedlack, and J. M. Doyle, Phys. Rev. Lett. **118**, 173201 (2017).
[37] N. Mukherjee and R. Zare, J. Chem. Phys. **135**, 024201 (2011).
[38] N. Mukherjee, W. Dong, and R. N. Zare, J. Chem. Phys. **140**, 074201 (2014).
[39] T. Scholak and P. Brumer, Adv. Chem. Phys. **162**, 39 (2017).
[40] T. Qureshi, Quanta **8**, 24 (2019).
[41] M. H. Alexander, D. E. Manolopoulos, and H.-J. Werner, J. Chem. Phys. **113**, 11084 (2000).
[42] N. Balakrishnan and A. Dalgarno, Chem. Phys. Lett. **341**, 652 (2001).
[43] C. Zhu, R. Krems, A. Dalgarno, and N. Balakrishnan, Astrophys. J. **577**, 795 (2002).
[44] V. Aquilanti, S. Cavalli, A. Simoni, A. Aguilar, J. M. Lucas, and D. De Fazio, J. Chem. Phys. **121**, 11675 (2004).
[45] V. Aquilanti, S. Cavalli, D. De Fazio, A. Simoni, and T. V. Tscherbul, J. Chem. Phys. **123**, 054314 (2005).
[46] V. Aquilanti, S. Cavalli, D. De Fazio, A. Volpi, A. Agular, and J. M. Lucas, Chem. Phys. **308**, 237 (2005).
[47] D. De Fazio, V. Aquilanti, and S. Cavalli, Front. Chem. **7**, 328 (2019).
[48] D. De Fazio, V. Aquilanti, and S. Cavalli, J. Phys. Chem. A **124**, 12 (2020).
[49] F. Lique, G. Li, H.-J. Werner, and M. H. Alexander, J. Chem. Phys. **134**, 231101 (2011).
[50] D. Skouteris, J. F. Castillo, and D. E. Manolopoulos, Comput. Phys. Commun. **133**, 128 (2000).
[51] K. Stark and H.-J. Werner, J. Chem. Phys. **104**, 6515 (1996).
[52] P. Staanum, S. D. Kraft, J. Lange, R. Wester, and M. Weidemüller, Phys. Rev. Lett. **96**, 023201 (2006).
[53] N. Zahzam, T. Vogt, M. Mudrich, D. Comparat, and P. Pillet, Phys. Rev. Lett. **96**, 023202 (2006).
[54] M. Viteau, A. Chotia, M. Allegrini, N. Bouloufa, O. Dulieu, D. Comparat, and P. Pillet, Science **321**, 232 (2008).
[55] G. Quéméner and P. S. Julienne, Chem. Rev. **112**, 4949 (2012).
[56] S. C. Althorpe and D. C. Clary, Annu. Rev. Phys. Chem. **54**, 493 (2003).
[57] Z. Ren, L. Che, M. Qiu, X. Wang, W. Dong, D. Dai, X. Wang, X. Yang, Z. Sun, B. Fu, S.-Y. Lee, X. Xu, and D. H. Zhang, Proc. Natl. Acad. Sci. USA **105**, 12662 (2008).
[58] D. H. Zhang and H. Guo, Annu. Rev. Phys. Chem. **67**, 135 (2016).